Interaction of two-level systems in amorphous materials with arbitrary phonon fields

D. V. Anghel,[1] T. Kühn,[2] Y. M. Galperin,[3,4,5] and M. Manninen[2]

[1]*National Institute for Physics and Nuclear Engineering-"Horia Hulubei," Street Atomistilor no. 407, P.O. Box MG-6, Bucharest-Magurele, Romania*

[2]*Nanoscience Center, Department of Physics, University of Jyväskylä, P.O. Box 35, FIN-40014 University of Jyväskylä, Finland*

[3]*Department of Physics and Centre of Advanced Materials and Nanotechnology, University of Oslo, P.O. Box 1048 Blindern, 0316 Oslo, Norway*

[4]*Argonne National Laboratory, 9700 S. Cass Avenue, Argonne, Illinois 60439, USA*

[5]*A. F. Ioffe Physico-Technical Institute of Russian Academy of Sciences, 194021 St. Petersburg, Russia*

To describe the interaction of the two-level systems (TLSs) of an amorphous solid with arbitrary strain fields, we introduce a generalization of the standard interaction Hamiltonian. In this model, the interaction strength depends on the orientation of the TLS with respect to the strain field through a 6×6 symmetric tensor of deformation potential parameters $[R]$. Taking into account the isotropy of the amorphous solid, we deduce that $[R]$ has only two independent parameters. We show how these two parameters can be calculated from experimental data, and we prove that for any amorphous bulk material, the average coupling of TLSs with longitudinal phonons is always stronger than the average coupling with transversal phonons (in standard notations, $\gamma_l > \gamma_t$).

PACS number(s): 63.50.+x, 61.43.Fs, 61.43.Er

I. INTRODUCTION

The thermal properties of dielectric crystals at low temperatures are well described by the Debye model. If the temperature is much smaller than the Debye temperature of the crystal, then the optical phonon modes are not excited and the only contribution to the heat capacity and heat conductivity comes from the acoustic phonons. In three-dimensional (3D) systems, low-frequency acoustic phonons have a linear dispersion relation, $\omega = c_{t,l}k$, where ω is the angular frequency, c_t and c_l are the transversal and longitudinal sound velocities, respectively, and k is the absolute value of the phonon's wave vector $\mathbf{k}$. This gives a specific heat proportional to the temperature to the power 3 ($c_V \propto T^3$).

A good estimate of the heat conductivity κ is $\kappa = \frac{1}{3}c_V cl$, where c is an average sound velocity and l is the phonon mean free path, which depends not only on the material but also on the sample quality. Impurities or lattice defects, even at low concentration, reduce the phonon mean free path and may thus decrease the heat conductivity dramatically.[1–4] As a result, the temperature dependence of the heat conductance is determined by the dependence of the phonon mean free path on its energy. Since such dependences can be very much different for different phonon-scattering mechanisms, the resulting temperature dependence of κ can be in general rather complicated.

In high-quality crystals of relatively small size and at sufficiently low temperature, the phonon mean free path may become comparable to or bigger than the crystal dimensions. In this case, the phonons scatter mainly at the surfaces and the mean free path is limited by the surface diffusivity and the geometrical features of the sample.[5] In this case, l is independent of the phonon frequency and $\kappa \propto c_V \propto T^3$.

By decreasing the temperature and the size of the system continuously, we get into the *mesoscopic* regime, where one or more dimensions of the system become comparable to the dominant phonon wavelength. Typically, we find this regime in nanometer-size objects, at temperatures of a few Kelvins or less. At such scales, the phonon interaction with the surfaces becomes important, since it leads to a coupling between different vibrational modes. This can lead to a very complicated set of phonon modes, with nonlinear dispersion relations. One example are the *Lamb modes*,[6] which are among the eigenmodes of a freestanding infinite membrane. Due to the advancement of nanotechnology, mesoscopic systems are used in more and more practical applications (see, for example, Refs. 7–14). The physical properties of mesoscopic devices can differ dramatically from those of bulk systems, the difference being more pronounced at lower temperatures.

Ultrathin freestanding membranes are important parts of many mesoscopic devices, such as microbolometers, electromechanical sensors, and actuators. The thermodynamics and thermal transport of such membranes are specifically important at low temperatures, where heat release is a bottleneck for device performance. At the same time, the low-temperature transport properties are rather unusual. For example, in many experiments the heat conductivity κ of large, thin membranes or long, narrow, and thin bridges is proportional to T^p, where p takes values between 1.5 and 2.[8–11] The specific heat of mesoscopic membranes is more difficult to measure. It can, however, be extracted from the amplitude of the temperature oscillations in ac measurements, and it appears also to be proportional to T^p, where p lies roughly between 1 and 2.[10]

The temperature dependence of κ and c_V in mesoscopic membranes and bridges can partly be explained by a crossover from a three-dimensional to a two-dimensional (2D) phonon gas distribution. This crossover takes place when the dominant thermal phonon wavelength, $\lambda_T = 2\pi\hbar c/k_B T$, is comparable to the membrane thickness.

Because of the finite thickness, there are gaps in the phonon spectra, the phonon dispersion relations near the band
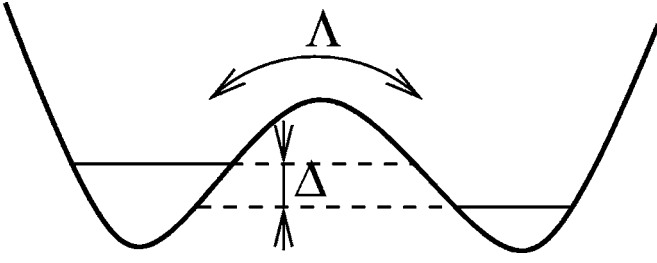
FIG. 1. An atom of a group of atoms moves in an effective potential like this. The separation between the ground states in the two wells, Δ, is much smaller than the energy scale of the oscillation frequency in the wells, ω_0.

edges being nonlinear. As a result, the temperature dependence of the specific heat deviates from the law $c_V \propto T^2$, which one would intuitively expect from a two-dimensional phonon gas. Instead, one obtains $c_V \propto T$ for very low temperatures.[10,11,13,15]

To study the heat conductivity in mesoscopic insulators, bridges have been cut out of the above-mentioned membranes. There, a decrease of the exponent of the temperature dependence of κ from 2 to about 1.5 was observed. Furthermore, the cut-off frequency of the temperature oscillations in ac heating measurements ($f_c \propto \kappa/c_V$) was observed to increase with temperature for the narrowest bridges.[10,16,17] Taking into account the fact that the edges of the bridges are very rough due to the cutting process, the measured data could be explained by using the dispersion relations of the above-mentioned Lamb modes to calculate heat capacity and heat conductivity.[13]

Nevertheless, in some experiments the same behavior, $\kappa \propto T^p$ with p being roughly 2,[9,10,14,16,17] and the increase of f_c with the temperature[10,16] were observed also above the 2D-3D crossover temperature. To explain these features, we have to extend our model and take into account the amorphous structure of the material—low stress amorphous silicon nitride—used in the above-mentioned experiments.

II. TWO-LEVEL MODEL

Amorphous or glassy materials differ significantly from crystals, especially in the low-temperature range, where for 3D bulks, $\kappa \propto T^2$ and $c_V \propto T$.[4,18] These temperature dependences were explained by the presence of specific dynamic defects. These defects are modeled by an ensemble of so-called *two-level systems* (TLSs) that exists in the material.[19,20] A TLS can be understood as an atom, or a group of atoms, which can tunnel between two close minima in configuration space, forming a hybridized doublet state. The presence of such minima is a hallmark of the glassy state. If the energy splitting between these minima is $\lesssim k_B T$, then the TLS can be excited from its ground state onto the upper level. In this way, the TLSs contribute to the heat capacity. TLSs can also scatter phonons and can thus decrease their mean free path and, correspondingly, the heat conductance.

An effective double-well potential and the tunneling of the atom between the two wells are depicted in Fig. 1.[19,20]

Written in the 2D Hilbert space spanned by the ground states of the two wells, the effective Hamiltonian of this TLS reads

$$H_{\mathrm{TLS}} = \frac{\Delta}{2}\sigma_z - \frac{\Lambda}{2}\sigma_x \equiv \frac{1}{2}\begin{pmatrix} \Delta & -\Lambda \\ -\Lambda & -\Delta \end{pmatrix}, \tag{1}$$

with Λ describing the tunneling between the two wells. In general, Δ is called the *asymmetry of the potential* and Λ is called the *tunnel splitting*. The Hamiltonian (1) may be diagonalized by an orthogonal transformation O,

$$H'_{\mathrm{TLS}} \equiv O^T H_{\mathrm{TLS}} O = \frac{\epsilon}{2}\sigma_z = \frac{1}{2}\begin{pmatrix} \epsilon & 0 \\ 0 & -\epsilon \end{pmatrix}, \tag{2}$$

where $\epsilon \equiv \sqrt{\Delta^2 + \Lambda^2}$ is the excitation energy of this TLS and the superscript T denotes in general *the transpose of a matrix*. Since the TLS can be in only two states, let us denote the ground state by $|\downarrow\rangle$ and the excited state by $|\uparrow\rangle$. Phonons at frequencies close to the level splitting ϵ are strongly scattered by TLSs.

The Hamiltonian parameters Δ and Λ are distributed with the density $VP(\Delta, \Lambda)$, where V is the volume of the solid. According to the standard tunneling model (STM), $P(\Delta, \Lambda)$ is assumed to have the form

$$P(\Delta, \Lambda) = P_0/\Lambda, \tag{3}$$

where P_0 is a constant. If expressed through the variables ϵ and $u \equiv \Lambda/\epsilon$, the distribution function is

$$P(\epsilon, u) = \frac{P_0}{u\sqrt{1 - u^2}}. \tag{4}$$

The strain caused by a phonon or any other kind of distortion of the material adds a perturbation to H_{TLS}, which we denote by H_1. The total Hamiltonian, $H = H_{\mathrm{TLS}} + H_1$, enables us to describe the coupling between a TLS and the phonon field. In the STM, the variation of the off-diagonal elements of H_{TLS} is neglected, so H_1 is diagonal,[18–22]

$$H_1 = \frac{1}{2}\begin{pmatrix} \delta & 0 \\ 0 & -\delta \end{pmatrix}. \tag{5}$$

The perturbation δ is linear in the strain field, S_{ij},[18,22] and in general may be written as $\delta \equiv 2\gamma_{ij}S_{ij}$. Here, as everywhere in this paper, we assume summation over repeated indices. The 3×3 symmetric strain tensor is defined as $S_{ij} = \frac{1}{2}(\partial_i u_j + \partial_j u_i)$, with u_i, $i=1,2,3$, being the components of the displacement field. According to Eq. (5), a static strain would just slightly renormalize the eigenvalues of the Hamiltonian. Since the thermal and transport properties of insulating solids are determined by lattice vibrations we are interested in the effect of a time-dependent strain entering the Hamiltonian H_1, which describes the interaction of the TLS with a phonon field. In such a situation, the interaction produces transitions of the TLS between its eigenstates in the unperturbed state. These direct transitions contribute to the phonon mean free path and thus influence the heat conductance.

The effect of the time-dependent modulation of the spacing between the TLS energy levels is very important for low-frequency phonons.[21] The populations of the TLS levels also change in time, but they lag behind the modulation of

the interlevel spacing. The resulting relaxation causes energy dissipation and, in turn, phonon damping. We do not consider this effect here since the heat conductance is governed by thermal phonons for which the resonant interaction is most important.

In the STM, the TLS interacts with 3D transversally or longitudinally polarized plane waves, which have all the components of the strain tensor proportional to the absolute value of the wave vector, k. The longitudinal wave will produce a compressional strain ($S_{yz}=S_{zx}=S_{xy}=S_{zy}=S_{xz}=S_{yx}=0$) and the transversal wave will produce a shear strain ($S_{xx}=S_{yy}=S_{zz}=0$). In this case, the expression for δ is always reduced to $\delta_\sigma=2N_\sigma\gamma_\sigma k_\sigma$, where $\sigma\equiv t$ or l denotes the transversal or longitudinal polarization of the wave, N_σ is the normalization constant of the phonon's displacement field, and γ_σ is called the *deformation potential parameter* or *coupling constant*. Since N_σ has dimensions of length, $N_\sigma k_\sigma$ is dimensionless and γ_σ has dimensions of energy. To calculate the transition rates of the TLS from one eigenstate to another, induced by the interaction with a phonon, we have to write H_1 in the basis that diagonalizes H_{TLS}:

$$H_1' \equiv O^T H_1 O = \frac{\delta}{2\epsilon}\begin{pmatrix} \Delta & -\Lambda \\ -\Lambda & -\Delta \end{pmatrix}. \tag{6}$$

The off-diagonal terms in H_1' determine the transition rates. Note that since the excitation and deexcitation of the TLS cause the absorption and emission of a phonon, respectively, δ is implicitly of the form $\delta\propto S_{\sigma k}b_{\sigma k}+\text{H.c.}$, where $b_{\sigma k}$ denotes a phonon annihilation operator. We omit this form here, but we shall use it explicitly in Sec. III B. To calculate the transition rates, let us denote the population of phonon modes by n and the population of excited TLS states by f. For example, in thermal equilibrium, $n_{k\sigma}=[e^{\beta\hbar\omega_{k\sigma}}-1]^{-1}$ and $f_\epsilon=[e^{\beta\epsilon}+1]^{-1}$, where $\beta=1/(k_B T)$. In these notations, the TLS deexcitation amplitude into a phonon of wave vector k and polarization σ, due to phonon-TLS interaction, is

$$\langle n_{k\sigma}+1,\downarrow|H_1'|n_{k\sigma}\uparrow\rangle = -\sqrt{\frac{\hbar k}{2V\rho c_\sigma}}\gamma_\sigma\frac{\Lambda}{\epsilon}\sqrt{n_{k\sigma}+1}. \tag{7}$$

Using Eq. (7), one obtains the contribution of a phonon with wave vector k and polarization σ to the TLS transition probability due to phonon emission and absorption, respectively:

$$\Gamma_{em}(\epsilon,\mathbf{k},\sigma) = \gamma_\sigma^2\frac{\pi k}{V\rho c_\sigma}\frac{\Lambda^2}{\epsilon^2}(n_{k\sigma}+1)\delta(\hbar c_\sigma k-\epsilon) \tag{8}$$

and

$$\Gamma_{abs}(\epsilon,\mathbf{k},\sigma) = \gamma_\sigma^2\frac{\pi k}{V\rho c_\sigma}\frac{\Lambda^2}{\epsilon^2}n_{k\sigma}\delta(\hbar c_\sigma k-\epsilon). \tag{9}$$

In the relaxation-time approximation, by summing $\Gamma_{abs}(\epsilon,\mathbf{k},\sigma)-\Gamma_{em}(\epsilon,\mathbf{k},\sigma)$ over all the phonon modes, we obtain the TLS relaxation time as [18,21]

$$\tau_\epsilon^{-1} = \left(\frac{\gamma_l^2}{c_l^5}+\frac{2\gamma_t^2}{c_t^5}\right)\frac{\Lambda^2\epsilon}{2\pi\rho\hbar^4}\coth\left(\frac{\beta\epsilon}{2}\right). \tag{10}$$

Similarly, we obtain the phonon relaxation time by summing over all the TLS states: [18,21]

$$\tau_{k\sigma}^{-1} = \frac{\pi\hbar\omega_{k,\sigma}}{\hbar\rho c_\sigma^2}\gamma_\sigma^2 P_0\tanh\left(\frac{\beta\hbar\omega_{k,\sigma}}{2}\right). \tag{11}$$

The low-temperature mean free path of a phonon in the amorphous material, $c_\sigma\tau_{k\sigma}$, can be determined from the so-called unsaturated ultrasound attenuation, i.e., from the attenuation of an external acoustic wave of such small amplitude so that only a small fraction of TLSs are excited out of equilibrium. From the acoustic attenuation, one can directly extract the product $\gamma_\sigma^2 P_0$. Another way to determine $\gamma_\sigma^2 P_0$ experimentally is by measuring the relative shift in the sound velocity: [18,23]

$$\frac{\Delta c_\sigma}{c_\sigma} = \frac{\gamma_\sigma^2 P_0}{\rho c_\sigma^2}\ln\left(\frac{T}{T_0}\right), \tag{12}$$

where T_0 is a reference temperature at which $\Delta c_\sigma=0$. Using these methods, Black calculated the product $\gamma_\sigma^2 P_0$. In fused silica, for example, its values are within the interval $(1.4-4.6)\times 10^7$ J/m^3 for longitudinal phonons and $(0.63-0.89)\times 10^7$ J/m^3 for transversal phonons, see Ref. 23 and references therein.

The values obtained for $\gamma_\sigma^2 P_0$ by these two independent methods can be combined to calculate the heat conductivity as

$$\kappa(T) = \frac{\rho k_B^3}{6\pi\hbar^2}\left(\frac{c_l}{\gamma_l^2 P_0}+\frac{2c_t}{\gamma_t^2 P_0}\right)T^2, \tag{13}$$

which can be measured by yet another experiment. [24]

Although sometimes there are pronounced differences between the values for $\gamma_\sigma^2 P_0$ obtained in different experiments (we are not concerned here with classification of results), it seems that $\gamma_l > \gamma_t$ always. To the best of our knowledge, this aspect is not explained in the literature. Moreover, the simplified expression for the perturbation term δ in the interaction Hamiltonian does not allow us to calculate the interaction of the TLS with an arbitrary strain field. Since, as mentioned above, the elastic modes in mesoscopic systems have rather complicated displacements and strain fields, we need a more general interaction Hamiltonian which should incorporate the microscopic symmetry of the material around the TLS and the orientation of the TLS with respect to the strain field. In the next section, we will build such an interaction Hamiltonian and, after we apply it to 3D bulk systems, we will show how we can extract information about its parameters from experiments. The relationship $\gamma_l > \gamma_t \geq 0$ is a natural result of our model. We will provide the results for the interaction between TLSs and Lamb modes in ultrathin membranes elsewhere.

III. THE GENERAL TLS-PHONON INTERACTION HAMILTONIAN

To generalize the TLS Hamiltonian, we shall use the full expression for δ of Eq. (5),

$$\delta = 2\gamma_{ij}S_{ij} \equiv 2[\gamma]:[S], \tag{14}$$

where γ_{ij} are the components of the 3×3 tensor $[\gamma]$ and ":" is the symbol for the dyadic product. Let us now find the general properties of $[\gamma]$.

Following Eq. (14), only the symmetric part of the tensor $[\gamma]$ has a physical meaning. Indeed, the dyadic product between a symmetric and an antisymmetric tensor is zero; so, the antisymmetric part of $[\gamma]$, even if existent, would not influence the results. We therefore assume $[\gamma]$ to be symmetric. Since all the tensors we have in our model are symmetric, it is more convenient to work using the *abbreviated subscript notation*, as described, for example, in Ref. 6. We will explain this method briefly.

Let us assume that $[A]$ is a symmetric 3×3 tensor (i.e., $A_{ij} = A_{ji}$). From its nine elements, only six are independent. To get rid of the redundant three elements and also to make the tensor manipulation easier, we can write $[A]$ in the form of a six component vector **A** in the following two ways:[6]

$$A_1 \equiv A_{xx}, \quad A_2 \equiv A_{yy}, \quad A_3 \equiv A_{zz},$$

$$A_4 \equiv A_{yz}, \quad A_5 \equiv A_{zx}, \quad A_6 \equiv A_{xy} \qquad (15)$$

or

$$A_1 \equiv A_{xx}, \quad A_2 \equiv A_{yy}, \quad A_3 \equiv A_{zz},$$

$$A_4 \equiv 2A_{yz}, \quad A_5 \equiv 2A_{zx}, \quad A_6 \equiv 2A_{xy}. \qquad (16)$$

Then, the dyadic product of two symmetric tensors, $[A]:[B]$, may be written as $[A]:[B] = \mathbf{A}^T \cdot \mathbf{B}$ if one of the tensors is written in form (15) and the other one in form (16). Applying this way of writing to Eq. (14), we define $\gamma \equiv (\gamma_{xx}, \gamma_{yy}, \gamma_{zz}, \gamma_{yz}, \gamma_{zx}, \gamma_{xy})^T$ and **S** $\equiv (S_{xx}, S_{yy}, S_{zz}, 2S_{yz}, 2S_{zx}, 2S_{xy},)$, so that $\delta = 2\gamma^T \cdot \mathbf{S}$.

As in Ref. 6, the subscripts in the abbreviated subscript notations will be denoted by capital letters, $I, J, K, \ldots$, which run from 1 to 6.

A. The properties of the deformation potential tensor

The vector γ should characterize the TLS and its deformability in the presence of a strain field. As explained before, the TLS is imagined as a particle or a group of particles that tunnels from one potential well to another. This tunneling may happen as a translation between the wells, or as a rotation.[25] In either case, there is a direction associated with the TLS, which we call $\hat{\mathbf{t}}$, for example, the direction defined by the two potential wells or the axis of rotation. One can expect that the orientation of the TLS (i.e., $\hat{\mathbf{t}}$ relative to the phonon's propagation direction and polarization has an effect on the interaction strength. The three components of $\hat{\mathbf{t}}$ are the only co(ntra)variant quantities that describe the TLS, from a very general point of view, i.e., without building a microscopic model of the TLS. With these quantities, we can construct the simplest symmetric 3×3 tensor,

$$[T] \equiv \begin{pmatrix} t_x^2 & t_x t_y & t_x t_z \\ t_x t_y & t_y^2 & t_y t_z \\ t_x t_z & t_y t_z & t_x^2 \end{pmatrix} = \hat{\mathbf{t}} \cdot \hat{\mathbf{t}}^T,$$

and a general one, $[\gamma] = [R]:[T]$ (i.e., $\gamma_{kl} = R_{ijkl} T_{ij}$), with $R_{ijkl} = R_{ijlk}$ for any k and l. We shall also choose $R_{ijkl} = R_{jikl}$ since the summation $R_{ijkl} T_{ij}$ allows us to use this simplifica-

tion. In abbreviated subscript notations, **T** $= (t_x^2, t_y^2, t_x^2, 2t_y t_z, 2t_z t_x, 2t_x t_y)^T$ and R_{ijkl} becomes R_{IJ} in an obvious way. Then, we can write γ as

$$\gamma \equiv [R]^T \cdot \mathbf{T}. \qquad (17)$$

Since **T** characterizes the orientation of the TLS, the relevant deformation potential parameters are contained in $[R]$. To make an analogy, the tensor $[R]$ is similar to the tensor of *elastic stiffness constants* from the elasticity theory. Still, the matrix $[R]$ cannot be taken arbitrarily. Like the elastic stiffness constants, the matrix $[R]$ is determined by the *local* symmetry properties of the atomic lattice, around the TLS. We will deduce here the properties of $[R]$.

We start by noting that the product $h_1 \equiv \mathbf{T}^T \cdot [R] \cdot \mathbf{S}$ is a scalar, so it should be invariant under any rotation of coordinates. Moreover, since $[R]$ reflects the microscopic symmetry of the lattice around the TLS, we shall do a sequence of transformations to obtain the properties of $[R]$. For the moment, let us assume that the lattice is simple cubic.

(1) Let us choose $S_1 = S_2 = S_3 = S_5 = S_6 = 0$, $S_4 \neq 0$, and $\hat{\mathbf{t}} = \hat{\mathbf{x}}$. Then, we rotate the coordinate system through π about the z axis. Under this rotation, $[R]$ is invariant, whereas **T** $= (t_x^2, 0, 0, 0, 0, 0)^T$ transforms into $\mathbf{T}' = \mathbf{T}$ and **S** $= (0, 0, 0, S_4, 0, 0)^T$ transforms into $\mathbf{S}' = -\mathbf{S}$. Then, $h_1 = \mathbf{T} \cdot [R] \cdot \mathbf{S} = R_{14} t_x^2 S_4 = \mathbf{T}' \cdot [R] \cdot \mathbf{S}' = -R_{14} t_x^2 S_4$ implies that $R_{14} = 0$. Performing similar rotations about the other axes of the coordinate system with appropriately chosen **T** and **S**, we can show that $R_{IJ} = 0$ for any $I = 1, 2, 3$ and $J = 4, 5, 6$.

(2) Taking **S** $= (S_1 \neq 0, 0, 0, 0, 0, 0)^T$ and **T** $= (0, t_y^2, t_z^2, 2t_y t_z, 0, 0)^T$ (so $t_x = 0$ and t_y, $t_z \neq 0$) and rotating the coordinate system through π about the z axis, we transform **S** into $\mathbf{S}' = \mathbf{S}$ and **T** into $\mathbf{T}' = (0, t_y^2, t_z^2, -2t_y t_z, 0, 0)^T$. From the product $h_1' = S_1 (R_{21} t_y^2 + R_{31} t_z^2 - R_{41} 2t_y t_z) = S_1 (R_{21} t_y^2 + R_{31} t_z^2 + R_{41} 2t_y t_z) = h_1$, we deduce that $R_{41} = 0$. Again, performing similar rotations about the other coordinate axes, we can show that $R_{JI} = 0$ for any $I = 1, 2, 3$ and $J = 4, 5, 6$. Up to now, we have proven that the matrix $[R]$ is block-diagonal. Let us see if we can simplify it further.

(3) Let us assume that $t_x = 0$, whereas t_y and t_z are different from zero. If from the components of the strain vector only S_5 is different from zero and we rotate the coordinates through π about the x axis, then $\mathbf{T} = (0, t_y^2, t_z^2, 2t_y t_z, 0, 0)^T \rightarrow \mathbf{T} = (0, t_y^2, t_z^2, 2t_y t_z, 0, 0)^T$ and $\mathbf{S} = (0, 0, 0, 0, S_5, 0) \rightarrow \mathbf{S}' = (0, 0, 0, 0, -S_5, 0)$. Calculating the products $\mathbf{T}^T \cdot [R] \cdot \mathbf{S}$ and $(\mathbf{T}')^T \cdot [R] \cdot \mathbf{S}'$, we find $R_{45} = 0$. By similar arguments, we conclude that $R_{45} = R_{46} = R_{56} = R_{54} = R_{64} = R_{65} = 0$.

(4) Due to the cubic symmetry, h_1 and H_1 should not depend on the notation of axes. Therefore, $R_{11} = R_{22} = R_{33}$, $R_{12} = R_{13} = R_{23}$, $R_{21} = R_{31} = R_{32}$, and $R_{44} = R_{55} = R_{66}$.

These are all the constraints that we can impose on $[R]$ if the lattice around the TLS has a cubic symmetry. Now let us make one more simplification and assume that the system is isotropic and find a relationship between the parameters R_{11}, R_{12}, R_{21}, and R_{44}.

Again, from the elasticity theory we know that both **T** and **S** transform under a rotation of coordinates like $\mathbf{T}' = [N] \cdot \mathbf{T}$

and $\mathbf{S}'=[N]\cdot\mathbf{S}$, where the matrix $[N]$ is defined, for example, on page 75 of Ref. 6. Since at a rotation of coordinates only $\mathbf{T}$ and $\mathbf{S}$ change, and not the deformation potential tensor (the interaction Hamiltonian should look the same in any coordinate system), $h_1=\mathbf{T}^T\cdot[R]\cdot\mathbf{S}=\mathbf{T}^T\cdot[N]^T\cdot[R]\cdot[N]\cdot\mathbf{S}$ for any $\mathbf{T}$ and $\mathbf{S}$. This implies $[R]=[N]^T\cdot[R]\cdot[N]$. Taking arbitrary rotations about each of the coordinate axes, we obtain the final conditions $R_{12}=R_{21}=R_{13}=R_{31}=R_{32}=R_{23}$ and $R_{11}-2R_{44}=R_{12}$.

By denoting $R_{11}\equiv\tilde{\gamma}$, $R_{12}/\tilde{\gamma}\equiv\zeta$, and $R_{44}/\tilde{\gamma}\equiv\xi$, we arrive at

$$[R]=\tilde{\gamma}\cdot\begin{pmatrix} 1 & \zeta & \zeta & 0 & 0 & 0 \\ \zeta & 1 & \zeta & 0 & 0 & 0 \\ \zeta & \zeta & 1 & 0 & 0 & 0 \\ 0 & 0 & 0 & \xi & 0 & 0 \\ 0 & 0 & 0 & 0 & \xi & 0 \\ 0 & 0 & 0 & 0 & 0 & \xi \end{pmatrix}\equiv\tilde{\gamma}\cdot[r], \quad (18)$$

with $\zeta+2\xi=1$.

The form of $[R]$ is very general. Yet, the parameters $\tilde{\gamma}$, ξ, and, implicitly, ζ may vary from one type of TLS to another. For example, for the two types of TLSs mentioned in the beginning of this section–translational and rotational (see Ref. 25 and references therein)–the parameters of $[R]$ may be different.

B. Physical results

We can now assemble back the expression for δ:

$$\delta=2\tilde{\gamma}\mathbf{T}^T\cdot[r]\cdot\mathbf{S}. \quad (19)$$

For the calculations of the physical quantities, we have to write H_1 in second quantization.[26] First, we introduce the excitation and deexcitation operators for the TLS,

$$a^{\dagger}=\begin{pmatrix} 0 & 1 \\ 0 & 0 \end{pmatrix}, \quad a=\begin{pmatrix} 0 & 0 \\ 1 & 0 \end{pmatrix}. \quad (20)$$

These matrix operators obey fermionic commutation relations and satisfy the conditions $\sigma_z=(2a^{\dagger}-1)$ and $\sigma_x=(a^{\dagger}+a)$. The phonon creation and annihilation operators are denoted by $b_{\mu}^{\dagger}$ and b_{μ}, respectively. Here, we use μ to denote general phonon modes. For 3D plane waves, $\mu\equiv(\mathbf{k}\sigma)$.

With these definitions, in the basis that diagonalizes H_{TLS}, the interaction Hamiltonian reads

$$\tilde{H}_1=\frac{\tilde{\gamma}\Delta}{\epsilon}\mathbf{T}^T\cdot[r]\cdot\sum_{\mu}[\mathbf{S}_{\mu}b_{\mu}+\mathbf{S}_{\mu}^{\star}b_{\mu}^{\dagger}](2a^{\dagger}a-1)$$

$$-\frac{\tilde{\gamma}\Lambda}{\epsilon}\mathbf{T}^T\cdot[r]\cdot\sum_{\mu}[\mathbf{S}_{\mu}b_{\mu}+\mathbf{S}_{\mu}^{\star}b_{\mu}^{\dagger}](a^{\dagger}+a), \quad (21)$$

where we used the notation $\tilde{H}_1$ to distinguish this form from Eq. (6). We denote by $\mathbf{S}_{\mu}$ the strain produced by the phonon field μ at the position of the TLS.

In the first-order perturbation theory, the matrix element for the absorption of a phonon $(\mathbf{k}\sigma)$ by an unexcited TLS is

$$\langle n_{\mathbf{k}\sigma},\uparrow|\tilde{H}_1|n_{\mathbf{k}\sigma}+1,\downarrow\rangle=-\frac{\tilde{\gamma}\Lambda}{\epsilon}\sqrt{\frac{\hbar n_{\mathbf{k}\sigma}}{2V\rho\omega_{\mathbf{k}\sigma}}}\mathbf{T}^T\cdot[r]\cdot\mathbf{S}_{\mathbf{k}\sigma}. \quad (22)$$

Applying Fermi's golden rule, we obtain the transition probability for this process. Assuming that the TLS directions are uniformly distributed in an amorphous solid, we sum the contributions of the TLSs, averaging over their directions, and we obtain an average transition rate,

$$\bar{\Gamma}_{|n_{\mathbf{k}\sigma},\uparrow\rangle,|n_{\mathbf{k}a}+1,\downarrow\rangle}=C_{\sigma}\tilde{\gamma}^2\frac{n_{\mathbf{k}\sigma}\pi k}{V\rho c_{\sigma}}\cdot\frac{\Lambda^2}{\epsilon^2}\delta(\hbar\omega_{\mathbf{k}\sigma}-\epsilon), \quad (23)$$

where C_{σ} is a constant that depends on the polarization of the phonon. Similarly, the emission rate is

$$\bar{\Gamma}_{|n_{\mathbf{k}\sigma}+1,\uparrow\rangle,|n_{\mathbf{k}\sigma},\downarrow\rangle}=C_{\sigma}\tilde{\gamma}^2\frac{(n_{\mathbf{k}\sigma}+1)\pi k}{V\rho c_{\sigma}}\cdot\frac{\Lambda^2}{\epsilon^2}\delta(\hbar\omega_{\mathbf{k}\sigma}-\epsilon). \quad (24)$$

Equations (23) and (24) are similar to Eqs. (9) and (8), respectively, with γ_t^2 replaced by $C_t\tilde{\gamma}^2$ and γ_l^2 replaced by $C_l\tilde{\gamma}^2$. The constants C_t and C_l are

$$C_l=\frac{1}{15}(15-40\xi+32\xi^2), \quad (25a)$$

$$C_t=\frac{4}{15}\xi^2. \quad (25b)$$

Even though we are not able to make any statement about the range in which ξ takes its value, we can still make the interesting prediction that

$$C_l>C_t\geq 0 \quad \text{for any } \xi, \quad (26)$$

in agreement with the experimental data.

The TLS relaxation time and phonon absorption time can still be calculated by Eqs. (10) and (11), with γ_t^2 and γ_l^2 replaced by $C_t\tilde{\gamma}^2$ and $C_l\tilde{\gamma}^2$. Therefore, $C_t\tilde{\gamma}^2$ and $C_l\tilde{\gamma}^2$ can be calculated from unsaturated ultrasonic attenuation or sound velocity shift experiments. Once the values $C_t\tilde{\gamma}^2$ and $C_l\tilde{\gamma}^2$ are obtained, the ratio

$$\frac{4C_l}{C_t}=\frac{15}{\xi^2}-\frac{40}{\xi}+32 \quad (27)$$

gives us the value of ξ, which further enables us to calculate ζ. If the value of $\tilde{\gamma}$ can be extracted from phonon-echo experiments,[27] then all the elements of the displacement potential tensor $[R]$ are known.

As a numerical example, we take from Ref. 23 the two sets of values for $P_0\gamma_l^2$ and $P_0\gamma_t^2$ that we used before. For the first one,[28] where $P_0\gamma_l^2=1.4\times 10^{-5}$ J/m^3 and $P_0\gamma_t^2=0.63\times 10^{-5}$ J/m^3, the two solutions for ξ are $\xi_1=0.55$ and $\xi_2=1.2$. Using the formula $P_0\tilde{\gamma}^2=P_0\gamma_t^2/C_t(\xi)$ [see Eq. (25b)] we obtain $(P_0\tilde{\gamma}^2)_1=7.8\times 10^7$ and $(P_0\tilde{\gamma}^2)_2=1.7\times 10^7$. For the second set of values[29]—$P_0\gamma_l^2=2.0\times 10^{-5}$ J/m^3 and $P_0\gamma_t^2=0.89\times 10^{-5}$ J/m^3—we get $\xi_1=0.55$ and $\xi_2=1.2$, which correspond to $(P_0\tilde{\gamma}^2)_1=11\times 10^7$ and $(P_0\tilde{\gamma}^2)_2=2.4\times 10^7$. Note that although $P_0\tilde{\gamma}^2$ (or $P_0\tilde{\gamma}_{\sigma}^2$) changes significantly from one

experiment to another, the ratio $P_0 \gamma_l^2 / P_0 \gamma_t^2$ does not change much, which leads to close values for the parameter ξ. From these measurements only, we cannot make the difference between ξ_1 and ξ_2.

IV. CONCLUSIONS

To describe the interaction of a TLS with an arbitrary strain field, we introduced a generalization of the standard TLS-plane wave interaction Hamiltonian. Such a generalization is useful in the description of mesoscopic systems, where the phonon modes are no longer the simple transversally and longitudinally polarized plane waves but have more complicated displacement fields and dispersion relations. We used the symmetry properties of the system to deduce the properties of our interaction Hamiltonian, $\tilde{H}_1$.

We showed that if the TLS is in an isotropic medium, then $\tilde{H}_1$ depends on four free parameters: two from the orientation of the TLS, $\hat{\mathbf{t}}$, and another two, denoted by $\tilde{\gamma}$ and ξ [Eq. (18)], which describe the coupling of the oriented TLS with the strain field. Since, in an amorphous solid, $\hat{\mathbf{t}}$ has random, uniformly distributed directions, the first two parameters are averaged and the effective form of the Hamiltonian has only two free parameters, $\tilde{\gamma}$ and ξ, like the Hamiltonian of the standard tunneling model. From sound absorption, sound velocity change, heat conductivity and phonon-echo experiments, one can calculate these two parameters, like we did in the end of the previous section.

On the other hand, if, for example, the distribution of the TLS orientations is not uniform, knowing the values of the parameters $\tilde{\gamma}$ and ξ, one can eventually reconstruct the distribution.

Different types of TLSs—translational and rotational ones—may have different deformation potential parameters. For one type of TLSs, we proved that $\gamma_l > \gamma_t$, which is confirmed by all the experimental results we know about.

[1] N. W. Ashcroft and N. D. Mermin, *Solid State Physics* (Harcourt College Publishers, Orlando, FL, 1976).

[2] Ziman, *Electrons and Phonons* (Oxford University Press, 2001).

[3] C. Kittel, *Introduction to Solid State Physics*, 7th ed. (Wiley, New York, 1996).

[4] R. C. Zeller and R. O. Pohl, Phys. Rev. B **4**, 2029 (1971).

[5] T. Klitsner, J. E. VanCleve, H. E. Fischer, and R. O. Pohl, Phys. Rev. B **38**, 7576 (1988).

[6] B. A. Auld, *Acoustic Fields and Waves in Solids*, 2nd ed. (Robert E. Krieger Publishing Company, Malabar, FL, 1990).

[7] T. J. Thornton, Rep. Prog. Phys. **58**, 311 (1995).

[8] F. Giazotto, T. T. Heikkilä, A. Luukanen, A. M. Savin, and J. P. Pekola, Rev. Mod. Phys. **78**, 217 (2006).

[9] W. Holmes, J. M. Gildemeister, P. L. Richards, and V. Kotsubo, Appl. Phys. Lett. **72**, 2250 (1998).

[10] M. M. Leivo and J. P. Pekola, Appl. Phys. Lett. **72**, 1305 (1998).

[11] D. V. Anghel, J. P. Pekola, M. M. Leivo, J. K. Suoknuuti, and M. Manninen, Phys. Rev. Lett. **81**, 2958 (1998).

[12] M. M. Leivo, A. J. Manninen, and J. P. Pekola, Appl. Supercond. **5**, 227 (1998).

[13] T. Kühn, D. V. Anghel, J. P. Pekola, M. Manninen, and Y. M. Galperin, Phys. Rev. B **70**, 125425 (2004).

[14] A. L. Woodcraft, R. V. Sudiwalaa, E. Wakui, R. S. Bhatia, J. J. Bock, and A. D. Turner, Physica B **284**, 1968 (2000).

[15] D. V. Anghel and M. Manninen, Phys. Rev. B **59**, 9854 (1999).

[16] M. Leivo, Ph.D. thesis, University of Jyväskylä, 1999.

[17] A. Luukanen, Ph.D. thesis, University of Jyväskylä, 2003.

[18] P. Esquinazi, *Tunneling Systems in Amorphous and Crystalline Solids* (Springer-Verlag, Berlin, 1998).

[19] W. A. Philips, J. Low Temp. Phys. **7**, 351 (1972).

[20] P. W. Anderson, B. I. Halperin, and C. M. Varma, Philos. Mag. **25**, 1 (1972).

[21] J. Jäckle, Z. Phys. **257**, 212 (1972).

[22] A. J. Leggett, S. Chakravarty, A. T. Dorsey, M. P. A. Fisher, A. Garg, and W. Zwerger, Rev. Mod. Phys. **59**, 1 (1987).

[23] J. L. Black, Phys. Rev. B **17**, 2740 (1978).

[24] R. B. Stephens, Phys. Rev. B **8**, 2896 (1973).

[25] Y. M. Galperin, V. G. Karpov, and V. I. Kozub, Adv. Phys. **38**, 669 (1989).

[26] D. V. Anghel and T. Kühn, cond-mat/0611528 (unpublished).

[27] B. Golding and J. E. Graebner, Phys. Rev. Lett. **37**, 852 (1976).

[28] B. Golding, J. E. Graebner, and R. J. Schutz, Phys. Rev. B **14**, 1660 (1976).

[29] B. Golding, J. E. Graebner, and A. B. Kane, Phys. Rev. Lett. **37**, 1248 (1976).